Electronic Supporting Information

Attaining air stability in high performing n-type phthalocyanine based organic semiconductors

Nathan J. Yutronkie,[1] Benjamin King,[2] Owen A. Melville,[2]
Benoit H. Lessard,[2,3,] and Jaclyn L. Brusso[1,*]*

[1]Department of Chemistry and Biomolecular Sciences, University of Ottawa, 150 Louis Pasteur, Ottawa, ON K1N 6N5, Canada

[2]Department of Chemical and Biological Engineering, University of Ottawa, 161 Louis Pasteur, Ottawa, ON K1N 6N5, Canada

[3]School of Electrical Engineering and Computer Science, University of Ottawa, 800 King Edward, Ottawa, ON, K1N 6N5, Canada

Contents (10 pages)

Theoretical Calculations.

As illustrated via DFT calculations to approximate the energies of the frontier molecular orbitals (FMOs) of **H_2-SiPc** juxtaposed to those of **F_2-SiPc**, axial fluorination has very little impact on the energetics (Figure S1). Incorporating 18 fluorine atoms, on the other hand, leads to a significant drop of the doubly degenerate LUMOs by nearly 1 eV, with an energy of -4.22 eV for the perfluorinated derivative **F_2-F_{16}SiPc**. Not only do these low-lying LUMOs suggest **F_2-F_{16}SiPc$_2$** to be an air-stable n-type OSC, but these energies are in close range to the work function of polycrystalline Ag electrodes (i.e., -4.26 eV), thus enhanced performances can be expected as a result of the minimization of the electron injection barrier.

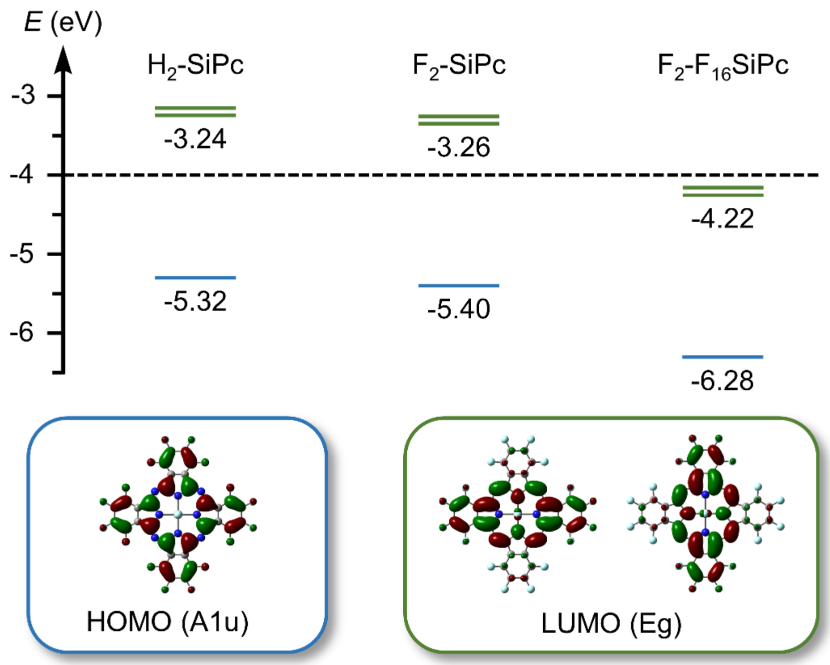

Figure S1. Energy level diagram of UB3LYP/6-311G(d,p) calculated HOMO and doubly degenerate LUMOs (as blue and green lines, respectively) from geometry optimized SiPc of D_{4h} symmetry (in eV). Dashed line corresponds to the LUMO energy threshold required for air stable electron transport performances in OSCs.

UV-Visible Spectroscopy.

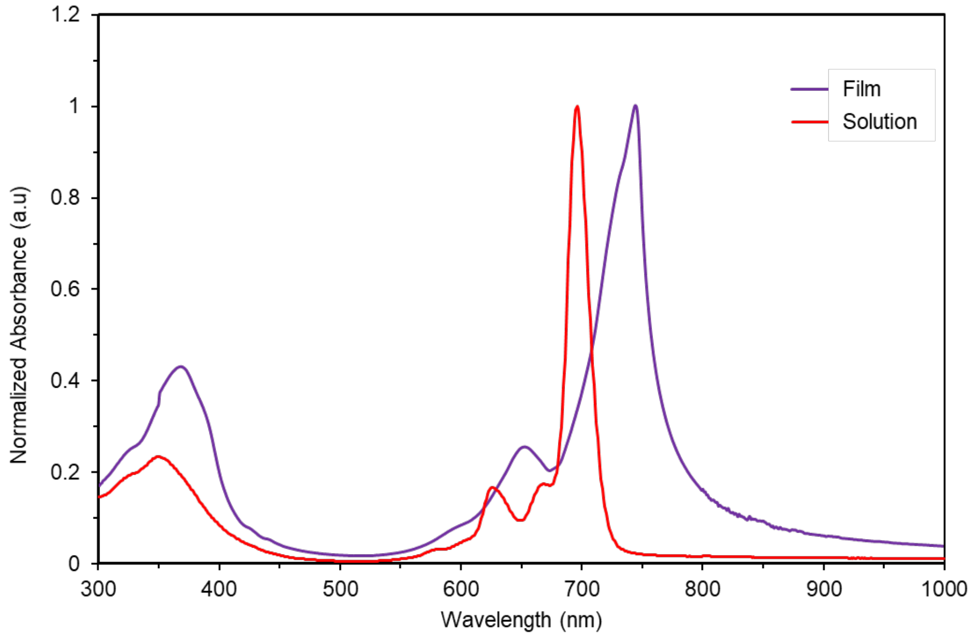

Figure S2. UV-Vis absorption spectra for **F_2-F_{16}SiPc** in solution (toluene) and as a thin film.

Single-Crystal X-Ray Diffraction.

Table S1. Crystallographic data for **F_2-F_{16}SiPc**.

Parameters	F_2-F_{16}SiPc
Formula	$C_{32}F_{18}N_8Si$
Formula Weight	866.49
Crystal System	Tetragonal
Space Group	$I4/_m$
a (Å)	14.8862(6)
b (Å)	14.8862(6)
c (Å)	6.2150(3)
α (°)	90
β (°)	90
γ (°)	90
V (Å^3)	1377.24(13)
Z	2
ρ_{calc} (g·cm^3)	2.089
T (K)	203(2)
μ (mm^{-1})	0.256
2θmax (°)	27.541
Total Reflections	866
Unique Reflections	795
R_1, wR_2 (on F^2)	0.0277, 0.0776

OTFT Testing and Electrical Characterization & Thin-Film X-ray Diffraction

Table S2. Electrical performances of OTFTs[a] using **F_2-F_{16}SiPc** and **F_{16}CuPc** as active layers characterized in N_2 and air.

Material	Condition	Dielectric	μ_e [$cm^2 \cdot V^{-1} \cdot s^{-1}$] [a]	V_T [V] [a]	I_{on} [A] [a]	$I_{on/off}$ [a]	μ_{max} [$cm^2 \cdot V^{-1} \cdot s^{-1}$]	n
F_2-F_{16}SiPc	N_2	OTS-SiO_2	0.15 ± 0.036	1.6 ± 0.52	9.34×10^{-5}	10^5–10^6	0.30	38
F_2-F_{16}SiPc	Air	OTS-SiO_2	0.072 ± 0.028	11.4 ± 2.1	3.76×10^{-5}	10^5	0.17	34
F_{16}CuPc	N_2	OTS-SiO_2	0.039 ± 0.014	3.2 ± 3.2	1.23 x 10^{-5}	10^4	0.063	31
F_{16}CuPc	Air	OTS-SiO_2	0.035 ± 0.013	3.3 ± 3.2	1.12 x 10^{-5}	10^5	0.061	31
F_2-F_{16}SiPc	N_2	SiO_2	0.025 ± 0.0087	-3.7 ± 2.5	1.67×10^{-5}	10^5	0.059	34
F_2-F_{16}SiPc	Air	SiO_2	0.0084 ± 0.0042	11.6 ± 2.0	3.24×10^{-6}	10^4–10^5	0.020	29
F_{16}CuPc	N_2	SiO_2	0.012 ± 0.0085	-0.2 ± 2.6	3.63 x 10-6	10^2–10^3	0.045	27
F_{16}CuPc	Air	SiO_2	0.010 ± 0.0085	-1.3 ± 2.7	2.9 x 10-6	10^3–10^4	0.040	26

[a)] Devices were fabricated using a BGTC architecture on Si/SiO_2 substrates with or without an OTS-modified dielectric layer and Ag source-drain electrodes.

[b)] μ_e and V_T were calculated based on mean values, while I_{on} and $I_{on/off}$ were calculated based on median values.

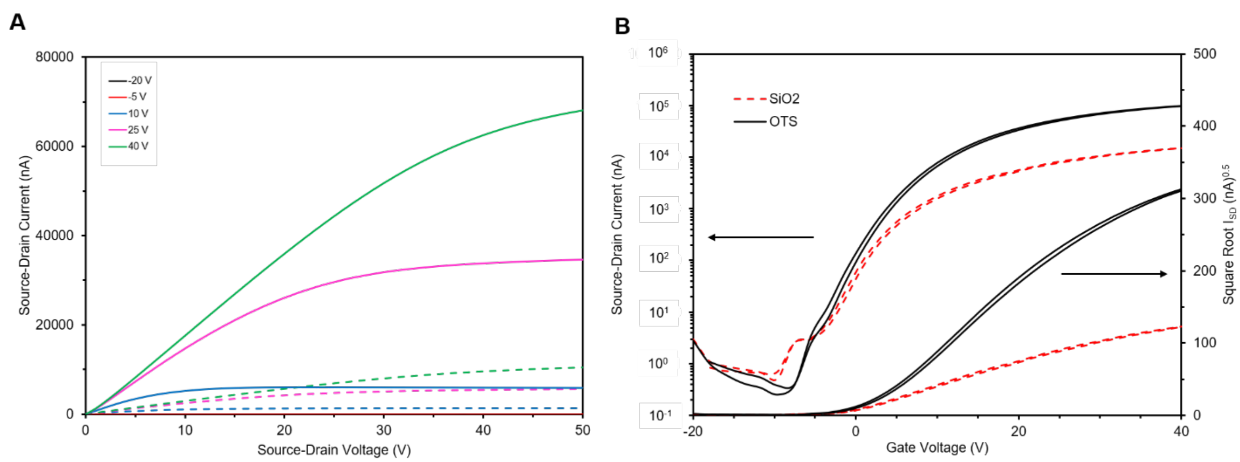

Figure S3. Representative (A) output and (B) transfer curves (V_{DS} = 50 V) for BGTC OTFTs fabricated with **F_2-F_{16}SiPc** characterized in an inert (N_2) atmosphere on OTS-modified SiO_2 (solid lines) and bare SiO_2 (dashed lines) as the dielectric

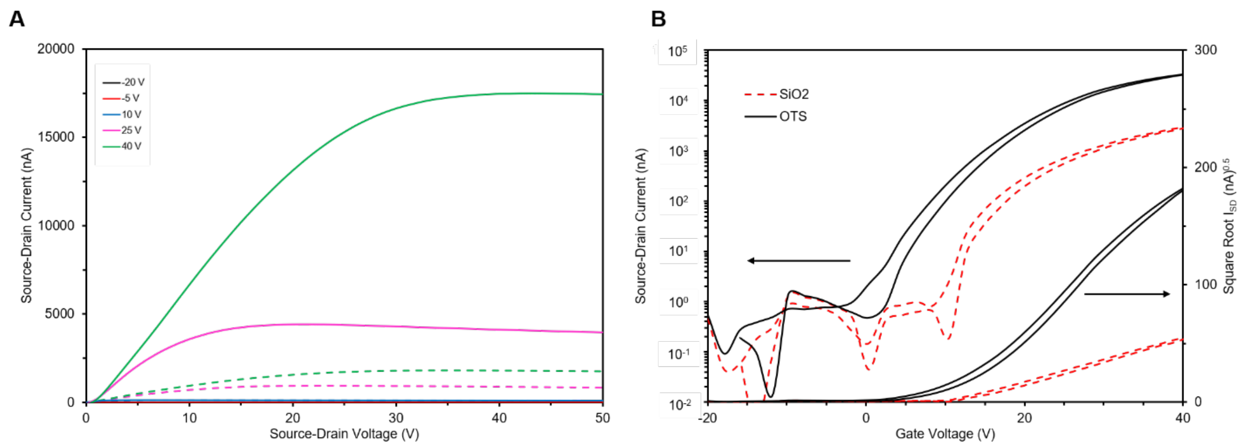

Figure S4. Representative (A) output and (B) transfer curves (V_{DS} = 50 V) for BGTC OTFTs fabricated with **F_2-F_{16}SiPc** characterized in air on OTS-modified SiO_2 (solid lines) and bare SiO_2 (dashed lines) as the dielectric

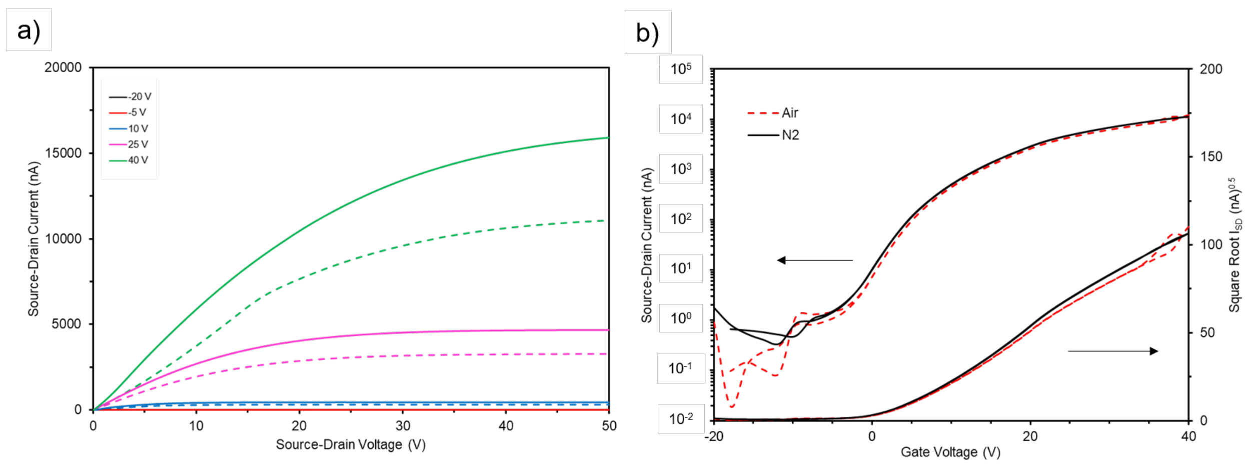

Figure S5. Representative (A) output and (B) transfer curves (V_{DS} = 50 V) for BGTC OTFTs fabricated with **F_{16}CuPc** on an OTS-modified substrate characterized in an inert (N_2) atmosphere (solid lines) and in air (dashed lines)

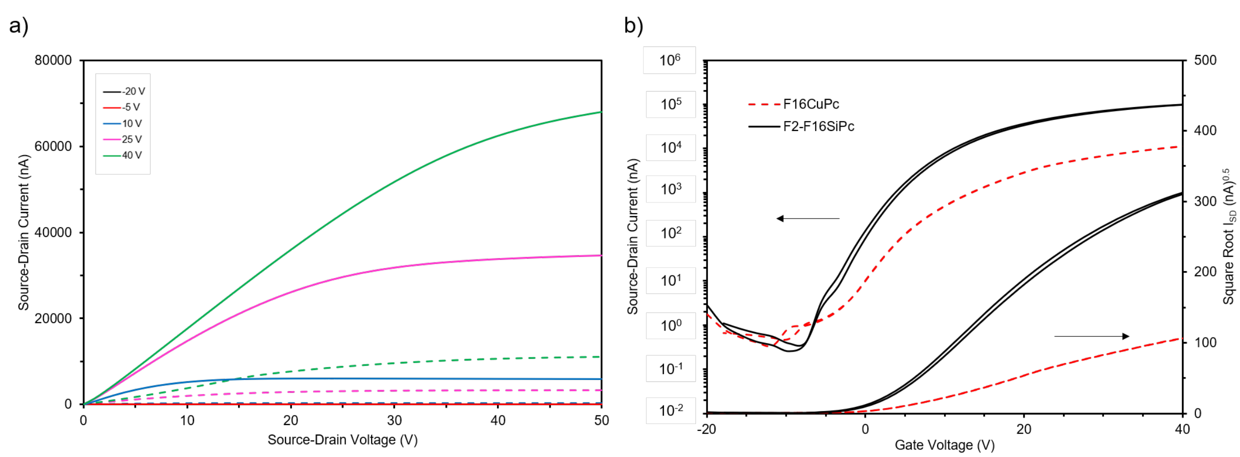

Figure S6. Representative (A) output and (B) transfer curves (V_{DS} = 50 V) for BGTC OTFTs fabricated with **F_2-F_{16}SiPc** (solid lines) and **F_{16}CuPc** (dashed lines) on an OTS-modified substrate characterized in an inert (N_2) atmosphere

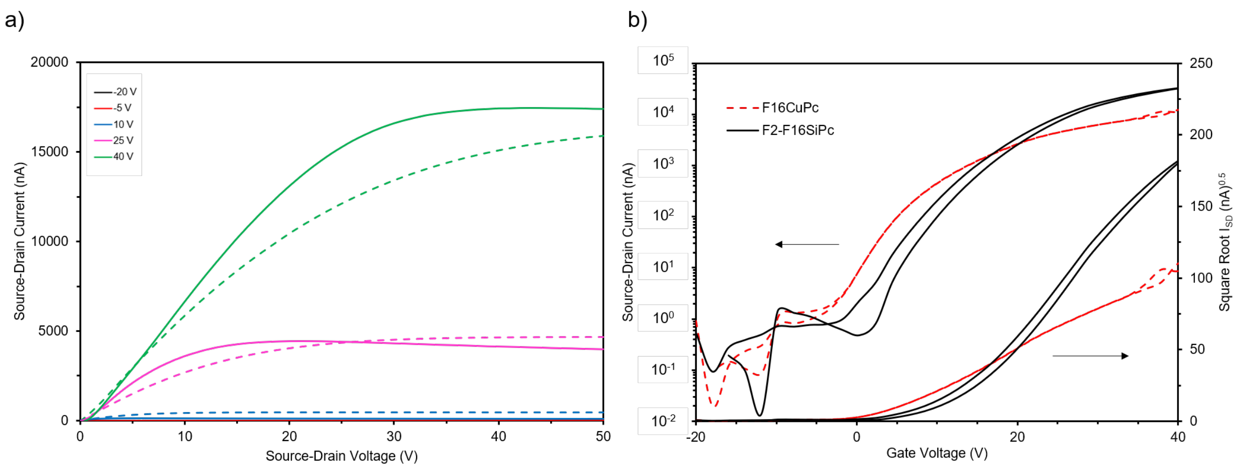

Figure S7. Representative (A) output and (B) transfer curves (V_{DS} = 50 V) for BGTC OTFTs fabricated with **F_2-F_{16}SiPc** (solid lines) and **F_{16}CuPc** (dashed lines) on an OTS-modified substrate characterized in air

Table S3. Electrical performance of **F_2-F_{16}SiPc** in BGBC device architectures with Au/ITO electrodes characterized in vacuum and air

Condition	Channel Length (μm)	μ_e x10^{-3} [$cm^2 \cdot V^{-1} \cdot s^{-1}$]	V_T [V]	I_{on} [A]	$I_{on/off}$
Vacuum		5.3 ± 1.2	2.1 ± 2.2	3.56 x10^{-6}	10^5
Air (t = 5 minutes)	20	3.7 ± 0.41	5.4 ± 1.2	2.23 x10^{-6}	10^4
Air (t = 6 months)		0.64 ± 0.39	12.1 ± 1.9	3.54 x10^{-7}	10^4
Vacuum		6.3 ± 2.4	-3.5 ± 2.7	9.28 x10^{-6}	10^5
Air (t = 5 minutes)	10	2.7 ± 1.5	3.7 ± 0.43	3.72 x10^{-6}	10^4-10^5
Air (t = 6 months)		0.54 ± 0.38	9.1 ± 1.5	4.45 x10^{-7}	10^4-10^5
Vacuum		7.8 ± 2.6	-2.3 ± 1.4	1.99 x10^{-5}	10^{5-}10^6
Air (t = 5 minutes)	5	3.3 ± 1.7	1.8 ± 2.7	1.05 x10^{-5}	10^4-10^5
Air (t = 6 months)		0.49 ± 0.44	4.6 ± 1.9	8.95 x10^{-7}	10^4-10^5
Vacuum		10.1 ± 4.2	-4.7 ± 0.60	7.35 x10^{-5}	10^4-10^5
Air (t = 5 minutes)	2.5	4.9 ± 0.81	0.19 ± 0.99	4.04 x10^{-5}	10^5
Air (t = 6 months)		0.54 ± 0.30	6.7 ± 0.74	2.81 x10^{-6}	10^4

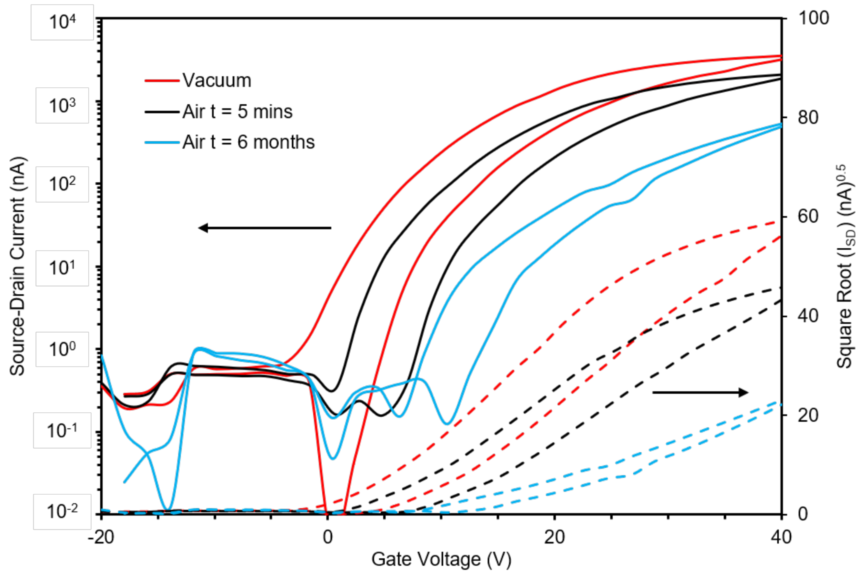

Figure S8. Representative transfer curves (solid lines) and $\sqrt{I_{SD}}$ vs V_G (dashed lines) for stability study of **F_2-F_{16}SiPc** in a BGBC architecture (V_{DS} = 50V) where L = 20 µm.

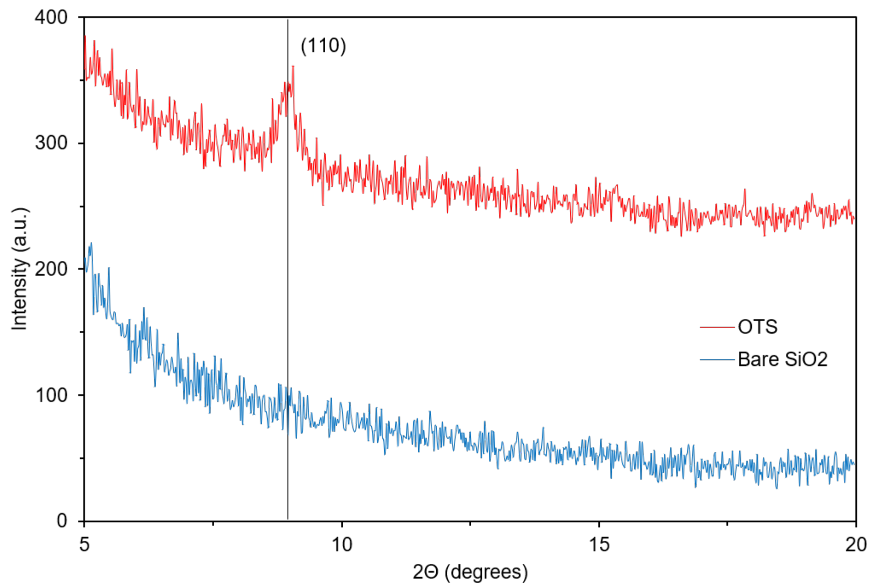

Figure S9 PXRD traces of **F_2-F_{16}SiPc** deposited on OTS and bare SiO_2 substrates with diffraction peak corresponding to the 110 plane of the single-crystal structure.

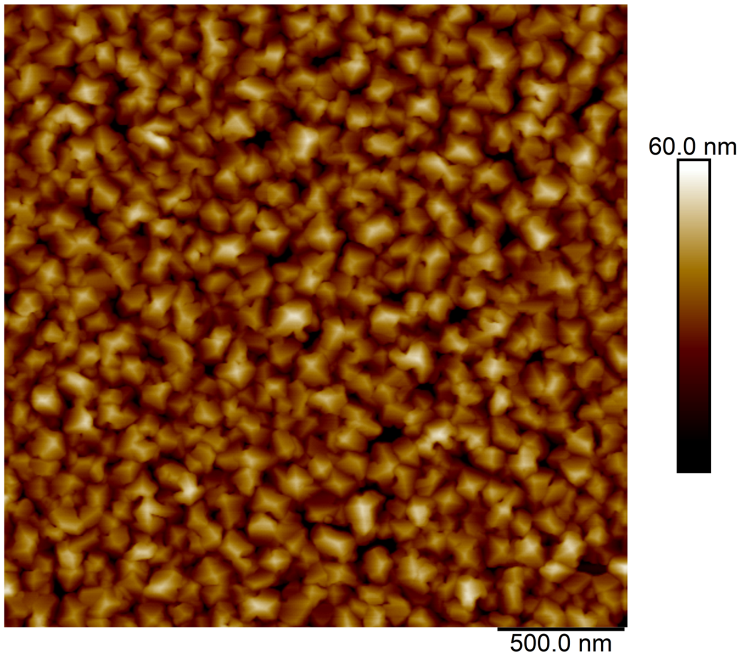

Figure S10. AFM image of **F_2-F_{16}SiPc** deposited on a bare SiO_2 substrate

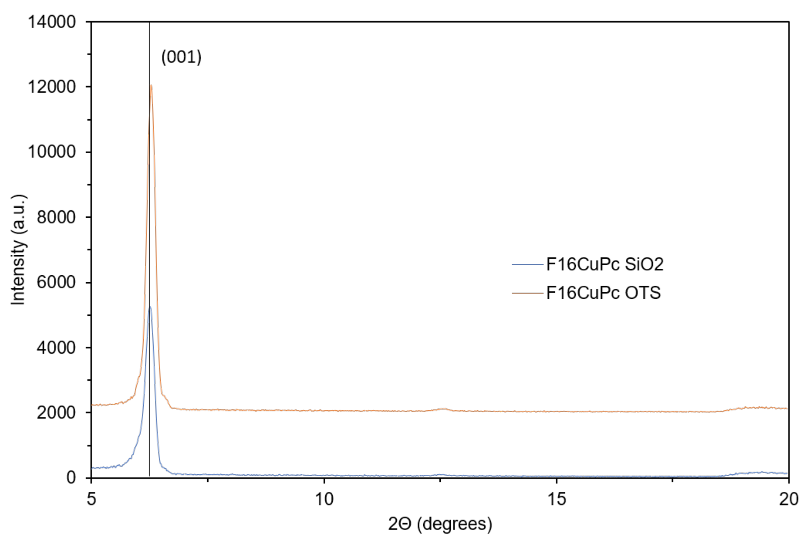

Figure S11. PXRD traces of **F_{16}CuPc** deposited on OTS and bare SiO_2 substrates with diffraction plane corresponding to the single crystal identified.